

# Physical modeling of spectral irradiance variations

J. Fontenla and G. Harder

LASP-Colorado Univ., Boulder, CO, USA; e-mail: fontenla@lasp.colorado.edu

**Abstract.** In this paper we introduce the Solar Radiation Physical Modeling (SRPM) methods and show its application to the modeling of spectral irradiance variations observed by the Spectral Irradiance Monitor (SIM) onboard SORCE. For the modeling we produce a set of seven physical models for features observed on the solar atmosphere. These models account for the available mid spatial and temporal-resolution observations of the main quiet-Sun and active-region features at visible and IR wavelengths. The computed, very high spectral resolution, spectra from each of these models at ten different positions on the disk are used together with image analysis of Precision Solar Photometric Telescope (PSPT) images to produce an image mask and the absolute spectral irradiance that corresponds to each set of PSPT images. After convolving the spectra with the specific instrumental profile one can directly compare these synthetic spectra with spectral irradiance observations. The combination of the models matches the observed solar irradiance measured by SOLSPEC within the combined observational and computational accuracy, but it is on the high side. Also, the spectral irradiance visible and IR are computed and convolved to SIM resolution for comparison or irradiance variations.

**Key words.** Sun:Irradiance – photosphere – chromosphere

## 1. Introduction

An important task to evaluate physical models of the various features of the solar atmosphere is the computation of the emitted spectrum at all relevant wavelengths and with good spectral resolution that allows for detailed comparison with observations. This was the goal of the methods described by Fontenla et al. (1999). The Solar Radiation Physical Modeling (SRPM) project expands this previous work and includes new technologies, and modules for computing full non-LTE and detailed radiative losses, apart from the modules

for computing the emitted spectrum. Thus, the system is intended not only for evaluating the radiative output of a given physical model but also for helping in the construction and diagnostic of such models based on semi-empirical methods or on more theoretical computations and simulations.

Physical models of the solar radiation consist of a set of physical parameters specified over a domain of the solar atmosphere that reproduce the observed emitted spectrum. This contrasts with empirical proxy-based models in which scaling formulas are used to try to relate intensities at various wavelengths. The semi-empirical models are constructed by matching observations of absolutely calibrated intensity

---

*Send offprint requests to:* J. Fontenla

and center-to-limb-variation (CLV). The early models, e.g. Gingerich and de Jager (1968) and Gingerich et al. (1971), aimed at evaluating the physical conditions in the solar photosphere by using local thermodynamic equilibrium (LTE) radiative transfer and medium-resolution observations. A set of quiet-Sun models was computed by Vernazza et al. (1981), hereafter VAL. The chromospheric extension was based on Skylab UV continuum and line intensity observations compiled by Vernazza & Reeves (1978). The transition region part of the model was based on those observations as an early attempt to explain the EUV line intensities from this region. The VAL models included an ad hoc temperature plateau at around 20,000 K to account for the Ly $\alpha$  line integrated intensity but did not match the detailed Ly $\alpha$  line profile or account for the energy balance in the transition region. Also, this set of models did not attempt to explain the observed He I lines. The VAL models considered the distribution of intensities from cell centers to bright network regions in the quiet Sun Skylab images, and consisted of a set of physical models labeled A through F to explain the observed distribution. Also, other chromospheric lines were considered such as the Ca II H and K and the Mg II h and k lines. However, although the integrated line intensity was consistent with the observations, the VAL detailed Ly $\alpha$  line profile was not consistent with observation because it had huge peaks and a very wide and deep central reversal completely different from that observed at high spectral (but moderate spatial and temporal) resolution by Fontenla et al. (1988). The theoretical transition region models by Fontenla et al. (1990, 1991, 1993), and Fontenla et al. (2002), hereafter FAL1, 2, 3, and 4, used the photospheric and chromospheric parts of the VAL models but replaced the arbitrary transition region at the footpoints of coronal loops by one derived from energy balance equations first considering particle diffusion of hydrogen (FAL 1 & 2), subsequently diffusion of both H and He (FAL 3), and finally mass flows in addition to diffusion (FAL 4). In addition, FAL modeling introduced additional models P and S that corresponded to bright plage and

sunspot umbra respectively. Several models exist for faculae, e.g., by Chapman (1977) and Walton (1987). We do not attempt to refer to all the research on these topics but point out that some models have been proposed that resort to complex geometrical effects and sub-resolution flux tubes to account for the center-to-limb-variation (hot wall models). The FAL model P considered the previous literature and adopted the semi-empirical 1-dimensional approach using a modified version of the Lemaire et al. (2001) model, and the umbra model is a modified version of the Maltby et al. model M. The models by Fontenla et al. (1999) derived from the FAL models and use FAL-type transition region models that depend only on the boundary conditions at the top of the chromosphere in which negligible local heating is assumed. However, such a simple scheme is not applicable to the chromospheric or coronal layers where local heating is important in balancing the radiative losses. Consequently they continue adopting a chromospheric structure inferred from available mid spatial-resolution observations but note that the data may not be enough to tightly constrain a physical model. These models introduced a model E somewhat similar to the corresponding in VAL, and a new model H for average plage that was intended to model the part of plage that is not visible as faculae at any disk positions except at the extreme limb.

In photospheric layers the radiative, and possibly convective, energy transport are essential and it can be argued that numerical simulations of magneto-convection should be able to explain the energy balance. While these simulations have been carried out by several researchers, there is not yet sufficient experimentation and analysis to be able to obtain reliable averages over medium spatial- and temporal-resolution spectra with adequate accuracy. Such averages are essential for understanding the solar irradiance. Besides, the simulations results are determined by the approximations made in regard to radiative transfer and by the boundary conditions (and sometimes the initial conditions) that are not well known. Also, local heating and incident radiations from above may also play a role in facu-

lae photospheres. Thus, until better proven results are obtained from simulations we use the semi-empirical photospheric models which are very well constrained by numerous observations and yield accurate emergent intensities.

## 2. SRPM system

The Solar Radiation Physical Modeling (SRPM) method is a modular system that allows for several evaluations concerning the radiation in any specified physical model of a feature of the solar atmosphere. One of its uses is for obtaining the resulting emergent spectrum at any direction as a result of specified parameters of a solar atmosphere. The computation of the emitted spectrum is based on Fontenla et al. (1999) but has been modified for using more up-to-date atomic data from NIST, HITRAN molecular data, and other sources. Also, the current system allows for using level populations obtained by methods other than the approximate non-LTE that Fontenla et al. (1999) used. Separate modules are now included in SRPM for computing the full non-LTE of many species in the solar atmosphere, including hydrogen with particle diffusion and Partial Redistribution (PRD). We are currently updating the atomic data so that all species level populations and ionization are computed in full non-LTE. The system now uses client/server techniques and several front-end modules designed for specific tasks, while all the modules are based on a common C++ class library. All input data are now stored in relational SQL databases and the NETCDF format is used for the output for portability reasons. The resolution of the computed spectrum covers in full detail each of the lines for which detailed atomic and molecular data is available. For this the spectral resolution is adjusted so that the line Doppler cores are covered by at least 20 points and the wings are covered by another 20 more spread points. A lower resolution is used to cover the continuum in the absence of lines. Our atomic data currently includes about 60,000 atomic lines from the NIST database, and several hundred thousand molecular lines from various sources (Gray and Corbally

1994, HITRAN, Kurucz CD, and others). These data as well as the atomic level and photoionization data are stored in the database and can be easily updated and inspected as new data becomes available, and in this way is decoupled from the code.

SRPM stores the atmospheric modes including elemental abundances in the SQL database and uses potentially variable elemental abundances. A separate database table contains the standard abundances from various sources including the latest values. These features allow for performing experiments with different values and variations of the elemental abundances whose results on the emitted spectrum can be readily computed by SRPM and evaluated comparing to observations. The various points in the atmosphere are characterized by a physical position (height in the 1-dimensional case, 1D), temperature, microturbulent velocity (for non-thermal line broadening), turbulent pressure velocity (for modification to the hydrostatic equilibrium), mass velocity (vertical in 1D), and by densities. These densities include the total hydrogen and the derived electron, proton, and neutral hydrogen densities and the H minus and H2 plus departure from LTE coefficients. The specification of each point is completed by the set of elemental abundances. We note that in this specification there are computed quantities and they are included here because they are initialized and can be computed and modified in a number of ways. Thus, by updating them from the relevant SRPM computations we are able to produce better isolated modules and still obtain and distribute to other investigators completely consistent results.

One key point of the SRPM system is that its computations of the non-LTE and the radiative losses are based on the Net Radiative Bracket Operator formulation that was used by Fontenla and Rovira (1985) and whose basis is partially described in Fontenla and Rovira (1985). This method was further developed to include PRD, and also particle diffusion and flows as outlined by Fontenla et al. (1996), Fontenla & Rovira (1985a), and Fontenla & Rovira (1985b). Although the current model atmospheres used are 1-dimensional, most

SRPM components can handle 3-dimensional models as well. We are now in the process of updating all the components for allowing full 3-dimensional computations. Our goal is to couple SRPM with available methods and code for MHD simulations (e.g., Collela et al. 2003) and in this way use better radiative losses in the dynamics simulations and more physically consistent models into the emergent radiation computation.

### 3. Current 1D model atmospheres

The current set of models for studying solar irradiance variations are described in detail by Fontenla et al. (2005), but an overview of their main achievements and issues is provided here. The 1D character of these semi-empirical and mid spatial-resolution models is due to the insufficient observations and statistics to constrain more complete 3D models that would base on higher resolution data, and the fact that at mid-resolution the 1D approximation can be justified by the small vertical extent of each of the regions (but although this argument is strong for the photosphere is less so for the chromosphere). Here we only discuss plane-parallel 1-dimensional models at medium resolution, in which such geometrical effects would only be relevant at the edges between different structures. Furthermore, we ignore the fluctuations within the resolution element and temporal variations, and thus the physical parameters in our models are radiation effective ones that correspond to the emitted radiation at the spatial resolution of a several arc-seconds and the temporal resolution averaged over p-modes and other fast dynamics. We find that 1D models such as those we study here can account for all current observations relevant to the spectral irradiance computations. However, these models do not explain some small details of the line spectra and also resort to ad hoc parameters such as the turbulent pressure velocity. More physically consistent models based on simulations, although very important for understanding the basic physical processes; have not yet proven their value for accurately evaluating the solar spectral irradiance variations. In order to produce synthetic solar spectral irradiances we

produce a discrete set of models that characterizes the solar disk on a given day. Our set includes 7 models corresponding to the main well known solar features that appear related to the magnetic fields observed in the photosphere. The set is as follows: 1) C for the interior of the network cells, 2) E for the medium brightness areas in the network lanes, 3) F for the active (bright) network, 4) H for plage that is not observable as faculae, 5) P for faculae, 6) S for sunspot umbra, 7) R for sunspot penumbra.

This set of models contains modified versions of 6 of the models in Fontenla et al. (1999), but now with updated abundances. The modifications we introduced in part because of the new abundances that are available in the literature and in part because of the consideration of new data about the contrast of the solar features with respect to quiet-Sun and the CLV of this contrast.

Models C and E correspond to quiet-Sun and model F is somewhat ambiguous because it may contain a solar activity component since the active network bright elements display magnetic element fluxes larger than the average network lanes. Sometimes it is possible to track active network to the byproduct of decay and fragmentation of active regions and it can be present in some degree even at the solar minimum phase of the activity. The other models are more clearly related to solar activity and the corresponding features are absent at solar minimum. Because of the insufficient observational constraints about absolute altitudes and because the  $\tau_{5000}=1$  level occurs most likely at different absolute altitudes in the Sun, the height scale of the individual models can be arbitrarily shifted and no relationship between the zero height in the various models exists. We currently prefer to characterize the temperature variation as a function of the gas pressure which is a local parameter of the gas and likely to be monotonic at least in the current photospheric and chromospheric layers. The current set of models is plotted in Fig. 1. In the present set of models we have dropped our previous model A that was used earlier to represent very dim portions of the network cell interior when observed in transition region lines. The reasons

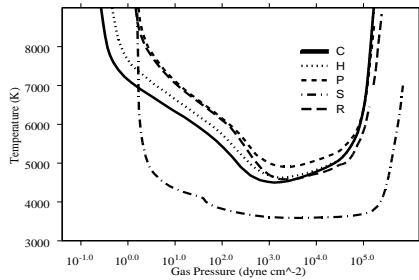


**Fig. 1.** Current 1D models.

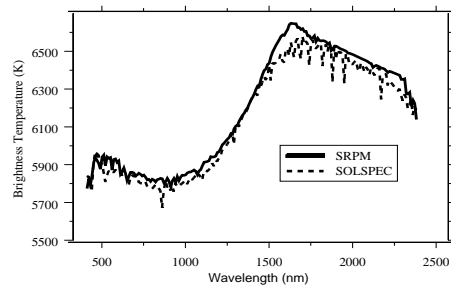


**Fig. 2.** Comparison of the observed and computed spectral irradiance brightness temperature, at 10 nm resolution.

for this are that: 1) it is not possible to identify this feature from available synoptic images such as the PSPT, 2) there is no clear signature of these regions in the visible and IR spectrum, 3) these regions are not important for the visible and IR irradiance and probably only marginal at most UV wavelengths, and 4) we have seen in UVSP observations in C IV that while most often these regions are observed in images at line center they seem to have significant red shifts and their dynamics is not well known.

Our current model C is identical to that in Fontenla et al. (1999), five of current models resulted from an update to the photospheres of the Fontenla et al. (1999) set of models, and a new model was created to represent sunspot penumbrae. We computed model C emitted radiation in the range 0.3 to 10 m using SRPM

for ten values of  $\mu$  and analyzed the center-to-limb-variation (CLV) of the red and IR continua, several well observed lines and the solar irradiance and found no good basis for introducing changes at this time. The continuum CLV corresponds very well to the observations by Pierce & Slaughter (1977a) and Pierce et al. (1977b) in the red and IR (at wavelengths not significantly affected by lines), and to the observed by the PSPT in the red band Fontenla et al. (2005). The Na I D, Mg I b, Ha, and many other lines correspond very well to the Kitt Peak data by Wallace et al. (1998). The absolute irradiance is slightly higher than the reported by Thuillier (2003) as is shown in Fig. 2, but within the combined observations and atomic data uncertainty.

The slightly higher irradiance resulting from our computations can be the result of unaccounted or incorrect data on photoionization cross-sections presently used by SRPM or it can result from incorrect abundances of some low first-ionization-potential (FIP) elements. Indeed, we notice that while many observed lines are very well matched by our computations some of them are not and we are investigating these mismatches to determine if they are likely to be due to incorrect atomic data or abundances. Also, since we will soon include better photoionization data we are waiting for these issues to settle before altering the previous model C to better match the absolute irradiance.

We found that the Fontenla et al. (1999) models E, F, and H display contrast with respect to model C,  $C_{\text{model}}(\mu, \lambda) = I_{\text{model}}(\mu, \lambda)/I_C(\mu, \lambda)$ , significantly above unity for red continuum wavelengths even at disk center and that this contrast is not observed. Thus, we revised the photospheres of models E, F, and H to remain identical to that of model C up to slightly higher altitudes than before. In the current models F and P have a contrast with respect to model C of only a small value above unity and only very close to the limb (model F less contrast than P). Although this appears consistent with observations we would like to have better observational constraints on the issue of active network and plage contrast in the continuum at several wavelengths. The photo-

sphere of model P for faculae was significantly changed and model S for umbrae was slightly changed to account for the observed contrast and its CLV in PSPT red band and published data. These changes were needed because the model S was not matching the published CLV data and model P was also not matching the observed contrast in the PSPT red band but displayed too high values. The changes for model P also took into account the IR contrast observed by Sanchez Cuberes et al. (2002). Note that we did not use the PSPT data for model S because of the uncertainties introduced by scattered light on these data. The photospheric layers of our new penumbrae model, R, considered the Kjeldseth-Moe & Maltby (1969), and del Toro Iniesta et al. (1994) photospheric modeling as well as PSPT red band data examined by us, and the published contrast and its CLV data.

The chromosphere and transition region in most of the current models are slightly modified versions of those from Fontenla et al. (1999) and will be updated soon to better match lower chromospheric observations and the data from chromospheric lines (e.g., the SUMER instrument on SOHO see Curdt et al. 2001). However, for model S we have significantly updated the upper chromosphere to account for the recent observations of the Ly continuum that indicate a much cooler but denser chromosphere than in our previous models (as is evidenced by the high intensity at the edge but faster decrease with decreasing wavelength). The chromosphere of the penumbra model was created to be similar to the plage model for accounting of observations in Ca II K3 and other lines that show the penumbra indistinguishable from surrounding plage at higher chromospheric lines. With the present computations of the spectra for all models (including model C) we find that updates to lower the  $T_{\min}$  in our models are necessary because our spectra calculations produce too weak molecular line absorptions (e.g., CN 3883 band and the G-band CH lines), and also because radio observations indicate a lower  $T_{\min}$  than the one in our current models. Also, an even lower  $T_{\min}$  was inferred from CO observations by Ayres and

Rabin (1996). Our present calculations use the current published abundances as summarized by Fontenla et al. (2005) and the calculations using the old abundance values give different results, thus, we are first addressing the issue of photospheric abundances in order to better constrain the future updates to the chromospheric and transition region models. We stress that updates to the abundances and the lower chromosphere temperatures have critical effects on the upper chromosphere and transition region models and thus it is better at this point to improve the models gradually from the bottom layers than to attempt changing the upper layers.

#### 4. PSPT image analysis

For the purpose of describing the effects on the spectral irradiance of the magnetic features observed on the solar disk we use the previously mentioned models together with masks of the solar disk. As is usual, these masks are pseudo images of the disk in which each pixel has a value (we use the index in the models listing above) corresponding to the feature that we identify at that pixel on solar disk images. For identifying the model for each pixel we analyze images in the red and the Ca II K bands obtained by the Precision Solar Photometric Telescope (PSPT, e.g. Vogler et al. 2005, <http://www.hao.ucar.edu/Public/research/fco.html>) operated at the M. Loa Observatory by the High Altitude Observatory. Although several methods exist in the literature, we have developed a different method that is akin to our models and the behavior observed and expected for the various solar features. Our method is relatively simple, fast, and produces very good results when stable image quality and filter bandpass are used. The PSPT red band is dominated by the continuum and contains only few photospheric lines and is used to identify sunspot umbra and penumbra. This is done by a simple contrast with respect to model C threshold between 0.9 and 0.7 for penumbra and below 0.7 for umbra. For evaluating this contrast we produce in each image a model C intensity in instrument units by decomposing the solar disk into a

set of 10 annuli and obtaining the median intensity value in the PSPT red band image. This median value is a good representation of model C because this component covers most of the area in all images and the median is better than the mean because it does not weight by the intensity. Each annuli median corresponds to the intensity for corresponding to the center-of-gravity of the annuli defined as in Fontenla et al. (1999). The function  $IC()$  is the cubic spline interpolation given by the points measured as indicated. For performance reasons we do not flatten the original red band image but instead for each pixel we just compute the contrast with respect to model C and compare with the thresholds for penumbra and umbra. If the pixel matches one of the thresholds the mask is assigned to that value in the corresponding pixel. This method works very well for umbra and penumbra because the observations indicate that these features contrast is nearly independent of the position on the disk, and certainly less variable than the intrinsic variations found on the features.

The PSPT Ca II K broad band image is selected for discriminating the other features because it contains the Ca II K3 spectral feature and because of its broadness displays a less variable, albeit small, network contrast. We certainly would like to use somewhat narrower bandpass images but the filter should be very stable with time (no wavelength shifts) and position on the image (same band for all points) or else complicated compensations would have to be performed. We use a more complicated threshold scheme for identifying the pixels other than umbra and penumbra because for the other solar features it is well established that the contrast with respect to model C is dependent on the disk position. Our scheme uses the expected contrast at each of the 10 positions in as given by the models and observations, and multiplies the expected contrast by the corresponding model C image intensities,  $IC(\mu)$ , derived as before but now for the Ca II K image. In this way we produce a set of functions (again using cubic spline interpolation) that describe the expected intensities for each of the features at each value of  $\mu$ . We then scan each pixel in the

Ca II K image, compare the image intensity value with the expected for all solar features at the corresponding  $\mu$ , and assign to the mask the index for the model which has an intensity closest to that measure at the pixel.

In this way we construct the image masks combining the features S and R from the red band image and the features C, E, F, H, and P from the Ca II K images. Of course the usual issues about image alignment and atmospheric refraction bring some problems close to the limb so we have to choose a cutoff value for relative radius,  $r = \sqrt{1 - \mu^2}$ , of 0.98 and assign model C to all pixels at radius between that cutoff and unity. The image masks are then used to compute the solar irradiance by averaging the computed intensities over all the pixels in the disk.

## 5. Conclusions

We described the SRPM system and some of its features and applications. One important application is for computation of the spectral irradiance based on a set of 1-D semi-empirical models of the main features observed on the solar disk and the analysis of PSPT red and Ca II K broad band images. The semi-empirical mid spatial-resolution models are obtained from analysis of many observations including continua and lines and at this point, except for model C, their photospheres have been improved to fit the CLV observations at many wavelengths in the visible and IR. A new model has been introduced for sunspot penumbra based, again, on observations. The chromospheres and transition regions of all models need improvements and a lowering of the temperature minimum value. Our method yields a daily synthetic irradiance spectrum that can be compared with observations by SOLSPEC and more recent ones by SIM. The absolute irradiances are consistent with those from Thuillier et al. (2003) within the combined observation and atomic data errors. The variations are broadly consistent with the described by Harder et al. (2005) but some differences appear that are described in that paper and point to necessary improvements in the set of models (e.g., Fontenla et al. 2004). Our

models and the full-resolution computed spectra, as well as degraded resolution spectra, for all models and 10 disk positions are available in <ftp://lasftp.colorado.edu/pub/fontenla/> and use our standard formats of text files for the models and NETCDF for spectra. More work is in progress for considering the latest photoionization data from Topbase, (e.g., Cowley and Bautista, M. 2003), atomic and molecular line data, and the computation of level populations of all species in full non-LTE. As new results are obtained we will update our ftp site to include them.

*Acknowledgements.* This work was supported by NASA contract NAS5-97045 at the University of Colorado.

## References

- Ayres, T. R., & Rabin, D. 1996, *ApJ*, 460, 1042  
 Chapman, G. A. 1977, *ApJS*, 33, 35  
 Colella, P., Graves, D.T., Ligocki, T.J., Martin, D.F., Modiano, D., Serafini, D.B., & Van Straalen, B. 2003, Chombo Software Package for AMR Applications, Lawrence Berkeley National Laboratory, Berkeley, CA  
 Cowley, C. R., & Bautista, M. 2003, *MNRAS*, 341, 1226  
 Curdt, W., Brekke, P., Feldman, U., Wilhelm, K., Dwivedi, B. N., Schhle, U., & Lemaire, P. 2001, *A&A*, 375, 591  
 del Toro Iniesta, J. C., Tarbell, T. D., & Ruiz Cobo, B. 1994, *ApJ*, 436, 400  
 Ding, M. D., & Fang, C. 1989, *A&A*, 225, 204  
 Fontenla, J.M., & Rovira, M. 1985a, *Journal Quant. Spec. Rad. Trans.*, 34, 389  
 Fontenla, J.M., & Rovira, M., 1985b, *Solar Phys.*, 96, 53  
 Fontenla, J., Reichmann, E. J., & Tandberg-Hanssen, E., 1988, *ApJ*, 329, 464  
 Fontenla, J. M., Avrett, E., & Loeser, R. 1990, *ApJ*, 355, 700 (FAL1)  
 Fontenla, J. M., Avrett, E., & Loeser, R. 1991, *ApJ*, 377, 712 (FAL2)  
 Fontenla, J. M., Avrett, E., & Loeser, R. 1993, *ApJ*, 406, 319 (FAL3)  
 Fontenla, J.M., Rovira, M., Vial, J.-C., & Gouttebroze, P. 1996, *ApJ*, 466, 496  
 Fontenla, J., White, O. R.; Fox, P. A.; Avrett, E. H.; & Kurucz, R. L. 1999, *ApJ*, 518, 480  
 Fontenla, J. M., Avrett, E., & Loeser, R. 2002, *ApJ*, 572, 636 (FAL4)  
 Fontenla, J. M., Harder, J., Rottman, G., Woods, T. N., Lawrence, G. M., & Davis, S. 2004, *ApJ*, 605, L85  
 Gingerich, O., & de Jager, C. 1968, *Sol. Phys.*, 3, 5  
 Gingerich, O., Noyes, R. W., Kalkofen, W., & Cuny, Y. 1971, *Sol. Phys.*, 18, 347  
 Gray, R.O., & Corbally, C. J. 1994, *AJ*, 107, 142  
 Harder, J., Lawrence, G. M., Fontenla, J. M., Rottman, G., & Woods, T. N. 2005, *Sol. Phys.*, in press  
 Kjeldseth-Moe, O., & Maltby, P. 1969, *Solar Phys.*, 8, 275  
 Kjeldseth-Moe, O., & Maltby, P. 1974, *Solar Phys.*, 36, 101  
 Lemaire, P., Gouttebroze, P., Vial, J.C., & Artzener, G.E. 1981, *A&A*, 103, 160  
 Maltby, P., Avrett, E. H., Carlsson, M., Kjeldset-Moe, O., Kurucz, R., & Loeser, R. 1986, *ApJ*, 306, 284  
 Pierce, A. K., & Slaughter, C. D., 1977a, *Solar Phys.*, 51, 25  
 Pierce, A. K., Slaughter, C. D., & Weinberger, W. 1977b, *Solar Phys.*, 52, 179  
 Sanchez Cuberes, M., Vazquez, M., Bonet, J. A. & Sobotka, M. 2002, *ApJ*, 570, 886  
 Thuillier, G., Herse, M., Labs, D., Foujols, T., Peetermans, W., Gillotay, D., Simon, P. C., & Mandel, H. 2003, *Sol. Phys.*, 214, 22  
 Vernazza, J. E., Avrett, E., & Loeser, R. 1981, *ApJS*, 45, 635 (VAL)  
 Vernazza, J. E., & Reeves, E. M. 1978, *ApJS*, 37, 485  
 Vogler, F.L., Brandt, P.N., Otruba, W., Hanslmeier, A. 2005, *Solar Magnetic Phenomena, Proc. 3rd Summerschool Solar Obs. Kanzelhhe, Austria (Aug. 25-Sept. 5, 2003)*. A. Hanslmeier, A. Veronig, and M. Messerotti (Edts.), *Astron. and Astrophys. Spa. Scie.* 320, 191, Springer  
 Wallace, L., Hinkle, K., & Livingston, W. 1998, *NSO Tech. Rep. #98-001*, National Solar Observatory.  
 Walton, S. R. 1987, *ApJ*, 312, 909